Vol. 19, n.° 1, pp. 103-108, 2020
Revista UIS Ingenierías
Página de la revista: revistas.uis.edu.co/index.php/revistauisingenierias

Amorphous gray iron for concrete reinforcement
Hierro gris amorfo para refuerzo de hormigón

Cosmin Codrean[1a], Mircea Vodă[1b], Dragoş Buzdugan[1c], Viorel Aurel Şerban[1d]

[1]University Politehnica Timişoara, Roumania. Orcid: [b] 0000-0002-0458-9217. Emails: [a] cosmin.codrean@upt.ro, [b] mircea.voda@upt.ro, [c] dragos.buzdugan@upt.ro, [d] viorel.serban@mec.upt.ro

Received: 20 February 2019. Accepted: 22 September 2019. Final version: 26 November 2019.

Abstract

Amorphous gray iron ribbons can be used as reinforcement fibers in the manufacture of composite materials due to a unique combination of high yield strength and a high hardness with good ductility. Amorphous ribbons with a thickness of 20 µm and width of 1.5 mm of $Fe_{73}Cr_8P_xSi_{12-x}C_7$ (x = 9, 10, 11) alloy were prepared by melt-spinning method. The elaborated alloys were structurally investigated by x-ray diffraction (XRD) and differential scanning calorimetry (DSC), while the mechanical properties were investigated by tensile microhardness and bending tests. It was found that increasing P content up to 10 atomic percentages led to a brittle material.

Keywords: amorphous gray iron ribbons; melt-spinning method; mechanical properties.

Resumen

Las cintas de hierro gris amorfo se pueden usar como fibras de refuerzo en la fabricación de materiales compuestos debido a la combinación única de alto límite elástico y alta dureza con buena ductilidad. Se prepararon cintas amorfas con un grosor de 20 µm y una anchura de 1,5 mm de aleación $Fe_{73}Cr_8P_xSi_{12-x}C_7$ (x = 9, 10, 11) mediante el método de hilado por fusión. Las aleaciones elaboradas se investigaron estructuralmente mediante difracción de rayos X (XRD) y calorimetría diferencial de barrido (DSC), mientras que las propiedades mecánicas se investigaron mediante micro dureza de tracción y pruebas de flexión. Se encontró que aumentar el contenido de P hasta 10 porcentajes atómicos condujo a un material quebradizo.

Palabras clave: cintas de hierro gris amorfo; método de hilado por fusión; propiedades mecánicas.

1. Introducción

Improvement of the mechanical characteristics of concrete by the addition of fibers (which are usually steel, glass or "plastic" fibers) is still in the focus of scientists [1, 2].

Compared to metal fibers, amorphous-metallic fiber offers higher mechanical strength.

A genre of corrosion- resistant amorphous metallic fibers (AMF) has been shown to have the ability to significantly enhance the flexural strength of concrete, even at relatively low dosages [3, 4].

Fe–Cr-Si alloys, due to their mechanical characteristics and good corrosion resistance, belong to the category of materials that can be used for reinforcement.

Incorporation of phosphorous (P) into Fe–Cr-Si alloys effectively enhanced the glass-forming ability (GFA) [5, 6], but at the same time increasing P content lead to an increase in hardness and tensile strength and decrease in ductility.

ISSN Printed: 1657 - 4583, ISSN Online: 2145 - 8456, **CC BY-ND 4.0**
How to cite: C. Codrean, M. Vodă, D. Buzdugan, V-A Şerban, "Amorphous gray iron for concrete reinforcement," *Rev. UIS Ing.*, vol. 19, no. 1, pp. 103-108, 2020. doi: 10.18273/revuin.v19n1-2020010

The costs of producing amorphous metallic materials only from pure elements are significantly higher than the production in combination with ferrous alloys.

The aim of our work was to produce an amorphous gray iron based on a combination between Fe, Cr, metals and Fe–C, Fe–P and Fe–Si ferroalloys and to analyze the influence of the content of P.

2. Experimental procedures

Ingots 10 mm in diameter and 30 mm in length of $Fe_{73}Cr_8P_xSi_{12-x}C_7$ (x = 9, 10, 11) (x = 9, 10, 11) (Figure 1) were prepared by induction melting the mixture of pure elements Fe, Cr, metals and Fe–C, Fe–P and Fe–Si ferroalloys in an argon atmosphere. The alloy compositions represent the nominal atomic percent. The master alloys were re-melted four times to obtain a better homogeneity.

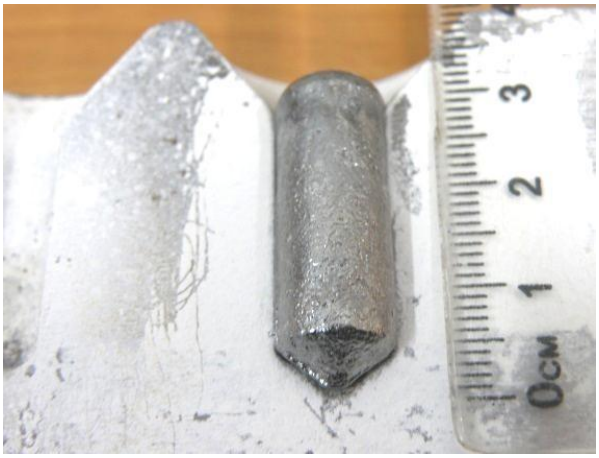

Figure 1. Ingot of master-alloy

Melt-spinning method was used to obtain the amorphous ribbons [7]. The optimal parameters for the fabrication of the amorphous ribbons are presented in Table 1.

Table 1. Optimal parameters for the ribbons elaboration

Parameters	Values
Melting temperature	1150 ºC
Cooling roller speed	2400 rot/min
Ejection nozzle sizes	ϕ 0.7 mm
Nozzle distance to cooling roller	0.8 mm
Overpressure applied to the melt	0.25 atm

Ductile, continuous, geometrically uniform ribbons of 20 μm thickness and 1.5 mm width were obtained. The macroscopic aspect of the obtained bands is shown in Figure 2.

The ribbons obtained are directly shaped and sized to be incorporated into cement mixtures, Figure 3.

Figure 2. Macroscopic aspects of the obtained ribbons

Figure 3. Amorphous fiber in the mixing stage with a cement-sand composition [1]

Structure of the elaborated ribbons was examined by x-ray diffraction, XRD, using an X'Pert³ Powder diffraction system, with the radiation of a Cu anode with a wavelength λ = 1.54 Å. The thermal stability of the amorphous ribbons was investigated by differential scanning calorimetry (DSC) using a Netzsch STA 441 Jupiter under a flow of purified nitrogen. The glass transition temperature Tg and the crystallization temperature Tx were determined as the onset temperatures of the glass transition and the crystallization peaks during heating with a constant rate of 0.33 K/s.

The mechanical properties were determined by the Vickers method micro-hardness test, tensile test, and bending tests. The hardness tests were performed using Volpert Micro - Vickers Hardness Tester with a 0.1 kgf load. The compressive tests were done at room temperature, at a loading speed of 1mm/min on a Zwick/Roell- machine. The bending test consists of determining the number of successive bends, until the appearance of cracks. At least 10 tests were performed to verify the accuracy and scatter of the data.

3. Results and discussion

The ribbons obtained by the melting-spinning method were structurally analyzed by x-ray diffraction. In the diffraction pattern (Figure 4) only broad peaks characteristic of an amorphous structure can be observed.

The DSC curves of the elaborated alloys of $Fe_{73}Cr_8P_xSi_{12-x}C_7$ (x = 9, 10, 11) are shown in Figure 5.

The presence of an exothermic peak which marks the crystallization event confirms the amorphous structure of the elaborated alloys. The glass transition temperature Tg and the crystallization temperature Tx for each alloy were determined and listed in Table 2.

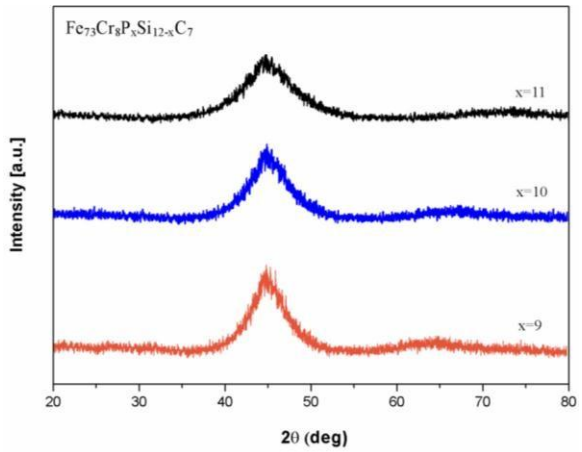

Figure 4. X-ray diffraction spectrums for the elaborated ribbons.

Also, $\Delta Tx = Tx-Tg$ parameter, which estimates the glass-forming ability (GFA), was calculated for each alloy. It is observed that with increasing the P content, the glass transition temperature Tg moves to lower values and the crystallization temperature Tx move to higher values. Consequently, the value of the ΔTx parameter increases, indicating an increase in GFA. This can be explained by the fact that P has a much smaller atomic radius than that of Fe and Cr, and therefore, by increasing the content of P an increasing of the atomic packing density of the liquid structure is favored [6]. The higher the atomic packing density, the easier it is to obtain the amorphous structure. Also, the presence of P in the chemical composition in Fe-based alloys contributes to a deoxidizing effect of the melt [8] which can lead to suppression of heterogeneous nucleation, thus improving the glass-forming ability.

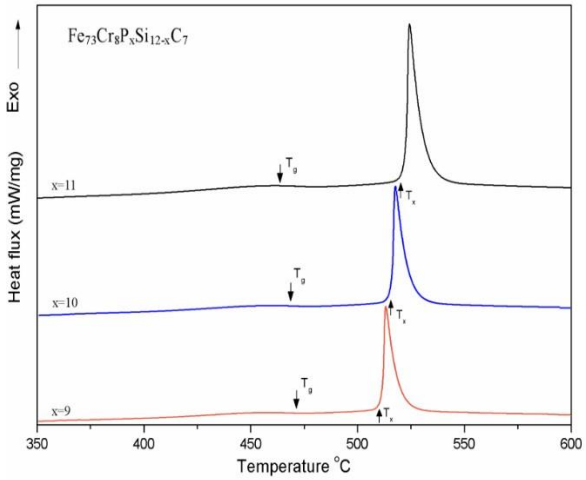

Figure 5. DSC curves of the elaborated ribbons

Table 2. Transformation temperatures for $Fe_{73}Cr_8P_xSi_{12-x}C_7$ amorphous alloys

Alloy / Temperatures	x=9	x=10	x=11
T_g[°C]	472	470	467
T_x[°C]	509	515	519
ΔT_x [°C]	37	45	52

Figure 6 presents the stress-strain curves for the as-cast $Fe_{73}Cr_8P_xSi_{12-x}C_7$ (x = 9, 10, 11) ribbons obtained by tensile tests. It can be observed that the stress-strain curves present a wider elastic deformation domain but also a smaller plastic deformation domain showing that it is a high resistance material. It is also noted that with the increase in P content, the plastic deformation domain is reduced.

Observation of the fracture zone by scanning electron microscope (Figure 7) reveals a typical fracture of amorphous alloys. It can be observed a smooth zone delimited by veins which is formed at the time of the fracture by moving of specific atoms and which explains the plastic deformation of the strips before breakage.

The microhardness values, ultimate tensile strength, yield stress and the number of bends are listed in Table 3.

It is found that the increase of the content in P leads to the increase of mechanical strength and hardness, while the bending ductility evaluated by the number of bends decreases.

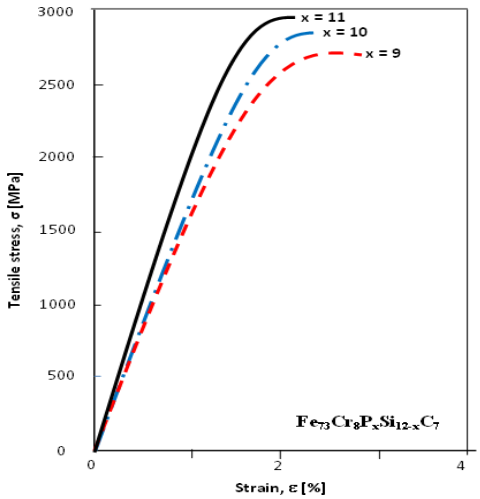

Figure 6. Stress-strain curves specific to the elaborated ribbons

The mechanical properties depend on the atomic size distribution and the chemical bonding between the atoms of the alloy elements. In principle, with increasing the atomic size distribution and chemical bonding strength the mechanical properties of resistance (hardness, ultimate tensile strength) increase and ductility decreases. The high values of the hardness and the ultimate tensile strength of these alloys are due to the presence in their chemical composition of the transition metals and the metalloids that form strong covalent bonds. Therefore, a higher content in P, which forms chemical compounds with Fe and Cr, increases the number of covalent bonds. On the other hand, a P higher atomic concentration leads to a wider atomic size distribution that favors a higher dense packing structure. The denser is the packing, the more covalent bonds are shorter and stronger and therefore the mechanical properties of resistance are higher [8].

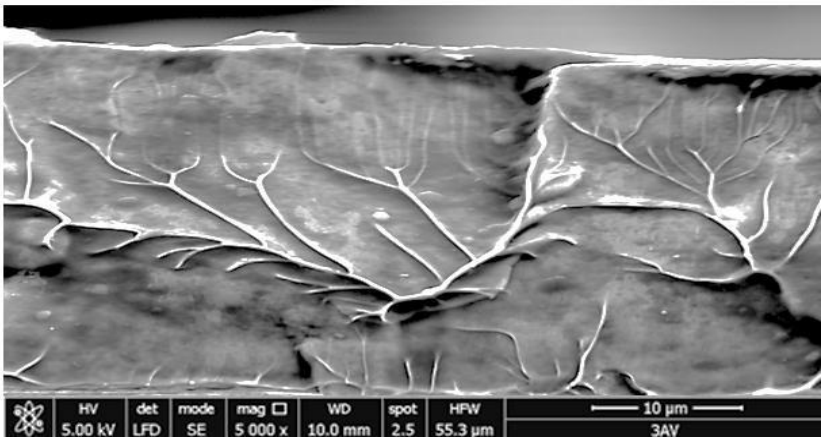

Figure 7 Fracture zone of the $Fe_{73}Cr_8P_{11}Si_1C_7$ ribbon

Table 3. Mechanical properties for $Fe_{73}Cr_8P_xSi_{12-x}C_7$ amorphous ribbons

Mechanical properties \ Alloy	X=9	X=10	X=11
Ultimate tensile strength., σ_f [MPa]	2760 ±25	2835 ± 30	2950 ± 22
Yield stress, σ_c [MPa]	2530 ± 20	2662 ± 25	2785 ± 18
Hardness, HV0.1	745 ± 10	763 ± 12	790 ± 10
Number of bends	53 ± 5	48 ± 6	41 ± 5

4. Conclusions

Amorphous Fe73Cr8PxSi12-xC7 (x = 9, 10, 11) ribbons of 20 μm thickness and 1.5 mm width have been successfully obtained by melt-spinning casting method. It was found the increase of the content in P leads to an increase in the supercooled liquid region ΔTx, which has the effect of improving the glass-forming ability of Fe-Cr-P-Si-C family alloys.

The mechanical tests showed that the elaborated amorphous ribbons are a high resistance material, but at the same time, the increase of the content in P leads to the increase of hardness, ultimate tensile strength and yield stress, while the bending ductility evaluated by the number of bends decreases.

In the range of variation of P content, in studied atomic percentages (9-11), it is found that an increase of 1% leads to an increase of 5 % in ultimate tensile strength and in yield stress, but up to 10% the material becomes brittle.

Generally, considering the mechanical properties of Fe-Cr-P-Si-C amorphous ribbons, they can be used as reinforcement fibers in the manufacture of concrete reinforcement.

References

[1] A. Cherkashin, Y. Begich, P. Sherstobitova, and O. Tolochko, "Amorphous fiber based on the Fe-B-C molten system for bulk reinforcement of concrete," *MATEC Web Conf.*, vol. 245, p. 03019, Dec. 2018, doi: 10.1051/matecconf/201824503019.

[2] K. Talantova, "Machine Building", *Proceedings of Higher Educational Institutions*, Rusia, 2014, pp. 99–106. doi: 10.18698/0536-1044

[3] S. K. Nayar and R. Gettu, "Benefits of using amorphous metallic fibres in concrete slabs-on-grade," *RILEM Tech. Lett.*, vol. 1, no. 0 SE-Articles, Dec. 2016, doi: 10.21809/rilemtechlett.2016.20.

[4] C. Jiang, Y. Wang, W. Guo, C. Jin, and M. Wei, "Experimental Study on the Mechanical Properties of Amorphous Alloy Fiber-Reinforced Concrete," *Adv. Mater. Sci. Eng.*, vol. 2018, 2018, doi: 10.1155/2018/2395083.

[5] Z. Li, S. Zhou, G. Zhang, and W. Zheng, "Highly Ductile and Ultra-Thick P-Doped FeSiB Amorphous Alloys with Excellent Soft Magnetic Properties," *Materials (Basel).*, vol. 11, no. 7, p. 1148, Jul. 2018, doi:10.3390/ma11071148.

[6] C. Wang *et al.*, "Effect of P on glass forming ability, magnetic properties and oxidation behavior of FeSiBP amorphous alloys," *Intermetallics*, vol. 84, pp. 142–147, 2017, doi: 10.1016/j.intermet.2016.12.024.

[7] D. Chicot *et al.*, "Mechanical properties of an Al91–Mn6–Nd3 nanostructured alloy," *Mater. Sci. Eng. A*, vol. 528, no. 22, pp. 7041–7051, 2011, doi: 10.1016/j.msea.2011.06.003.

[8] H. X. Li, Z. C. Lu, S. L. Wang, Y. Wu, and Z. P. Lu, "Fe-based bulk metallic glasses: Glass formation, fabrication, properties and applications," *Prog. Mater. Sci.*, vol. 103, pp. 235–318, 2019, doi: 10.1016/j.pmatsci.2019.01.003.